HHS Public Access

Author manuscript

AIDS. Author manuscript; available in PMC 2016 October 31.

Published in final edited form as:

AIDS. 2015 July 31; 29(12): 1445–1457. doi:10.1097/QAD.0000000000000739.

Monocytes from HIV+ individuals show impaired cholesterol efflux and increased foam cell formation after transendothelial migration

Anna MAISA[1], **Anna C. HEARPS**[1,2], **Thomas A. ANGELOVICH**[1,3], **Candida F. PEREIRA**[1,2,4], **Jingling ZHOU**[1], **Margaret D.Y. SHI**[1,5], **Clovis S. PALMER**[1], **William A. MULLER**[6], **Suzanne M. CROWE**[1,2], and **Anthony JAWOROWSKI**[1,2,7,*]

[1]Centre for Biomedical Research, Burnet Institute, Melbourne, VIC, Australia

[2]Department of Infectious Diseases, Monash University, Melbourne, VIC, Australia

[3]School of Applied Sciences, RMIT University, Melbourne, VIC, Australia

[4]Monash Micro Imaging, Monash University, Melbourne, VIC, Australia

[5]Department of Microbiology and Immunology, Melbourne University, Melbourne VIC, Australia

[6]Feinberg School of Medicine, Northwestern University, Chicago, IL, USA

[7]Department of Immunology, Monash University, Melbourne, VIC, Australia

Abstract

Design—HIV+ individuals have an increased risk of atherosclerosis and cardiovascular disease which is independent of antiretroviral therapy and traditional risk factors. Monocytes play a central role in the development of atherosclerosis, and HIV-related chronic inflammation and monocyte activation may contribute to increased atherosclerosis, but the mechanisms are unknown.

Methods—Using an *in vitro* model of atherosclerotic plaque formation, we measured the transendothelial migration of purified monocytes from age-matched HIV+ and uninfected donors and examined their differentiation into foam cells. Cholesterol efflux and the expression of cholesterol metabolism genes were also assessed.

Results—Monocytes from HIV+ individuals showed increased foam cell formation compared to controls (18.9% vs 0% respectively, p=0.004) and serum from virologically suppressed HIV+ individuals potentiated foam cell formation by monocytes from both uninfected and HIV+ donors. Plasma TNF levels were increased in HIV+ vs control donors (5.9 vs 3.5 pg/ml, p=0.02) and foam cell formation was inhibited by blocking antibodies to TNF receptors, suggesting a direct effect on

*corresponding author: A/Prof Anthony Jaworowski, Centre for Biomedical Research, Burnet Institute, 85 Commercial Rd, Melbourne, VIC, Australia 3004. anthonyj@burnet.edu.au, Phone: +61 3 9282 2127.

Author contributions

AM, AH, TA, CP, JZ and MS generated experimental data for this study in the laboratory of SC and AJ; CP, SC, WM and AJ had input into study design, whilst AM, CP, AH and AJ performed data analysis and manuscript preparation.

Conflicts of interest

The authors declare no conflicts of interest.

monocyte differentiation to foam cells. Monocytes from virologically suppressed HIV+ donors showed impaired cholesterol efflux and decreased expression of key genes regulating cholesterol metabolism, including the cholesterol transporter ABCA1 (p=0.02).

Conclusions—Monocytes from HIV+ individuals show impaired cholesterol efflux and are primed for foam cell formation following trans-endothelial migration. Factors present in HIV+ serum, including elevated TNF levels, further enhance foam cell formation. The pro-atherogenic phenotype of monocytes persists in virologically suppressed HIV+ individuals and may contribute mechanistically to increased atherosclerosis in this population.

Keywords

HIV; foam cells; monocytes; macrophage; atherosclerosis; cholesterol efflux; innate immune activation

INTRODUCTION

Cardiovascular disease (CVD) is an increasing cause of morbidity and mortality in HIV+ individuals receiving combination antiretroviral therapy (cART) [1, 2]. HIV infection is associated with an increased risk of cardiovascular conditions including atherosclerosis [3, 4] and coronary heart disease [5, 6] and an approximately two-fold increased risk of myocardial infarction [7, 8]. Importantly, increased CVD risk in HIV+ individuals is independent of traditional risk factors [5–10] and risk prediction algorithms based on these factors alone used in the general community setting underestimate atherosclerosis in HIV+ individuals [11]. Whilst cART and specific antiretroviral agents may potentiate CVD [12–14], the increased CVD risk observed in HIV+ individuals who are treatment naïve [13], undergoing treatment interruption [15] and in elite controllers [16] suggests the involvement of cART-independent factors. Taken together, these observations suggest that unique mechanisms exist in HIV+ individuals which act in addition to traditional factors to increase CVD risk, and these effects persist despite viral suppression.

In HIV+ individuals, CVD is associated with markers of inflammation [17–19] and is increasingly reported in association with markers of monocyte/macrophage activation. We have shown that monocyte and innate immune activation persist in HIV+ individuals despite viral suppression [20, 21], and markers of monocyte/macrophage activation including soluble (s)CD163 [22, 23], sCD14 [24] and cellular monocyte activation markers [25–27] are associated with atherosclerosis and CVD in HIV infection. Despite the significant links between chronic inflammation/monocyte activation and increased CVD risk in HIV infection, the mechanism remains unclear.

Pro-inflammatory cytokines such as TNF potentiate atherosclerosis; they activate endothelial cells and monocytes, resulting in increased expression of adhesion molecules, release of chemoattractants by endothelial cells, lipid transcytosis and oxidation of low density lipoprotein (LDL) [28]. Activated monocytes are recruited to inflamed blood vessels and migrate into the vascular neointima, where they endocytose lipids and either exit via reverse transendothelial migration or develop into foam cells by phagocytosing highly inflammatory oxidized LDL (oxLDL; via scavenger receptors SR-A and CD36) [29]. Foam cells have

reduced migratory capacity [30] and accumulate in the neointima where they release pro-inflammatory molecules contributing to further recruitment of monocytes and progression of atherosclerosis [31]. The ability of macrophages to exit the neointima and remove cholesterol via reverse transendothelial migration is critical to retarding the development of atherosclerotic plaques and promoting plaque regression [32].

We hypothesized that monocyte activation in the setting of chronic HIV infection [20] promotes atherosclerosis. We have previously developed a novel *in vitro* model of the initiation of atherosclerotic plaque formation that couples transendothelial migration of primary human monocytes across an activated endothelium with foam cell formation [33–35]. Here, we adapted this model to investigate the atherogeneic potential of monocytes isolated from HIV+ individuals and determine whether inflammatory factors elevated in HIV infection influence early atherosclerotic events mediated by monocytes.

METHODS

Recruitment and blood processing

Blood was obtained from HIV+ donors recruited from the Department of Infectious Diseases, The Alfred Hospital, Melbourne, Australia and healthy control donors of a similar age following written, informed consent. Peripheral blood mononuclear cells (PBMCs) were isolated within 2 hours of sample collection and were either used immediately (for migration assays) or stored in liquid nitrogen for later mRNA and cholesterol efflux analysis. Monocytes were further purified from PBMC via negative selection using magnetic beads (Miltenyi Biotec, Cologne, Germany) as per the manufacturer's protocol, which yields monocytes with a purity of 80–85% as determined by flow cytometry (not shown). This study received ethical approval from The Alfred Research and Ethics Committee and from the Royal Women's Hospital Ethics Committee, Melbourne.

Cell migration assay and analysis

Hydrated collagen gels were prepared in a 96-well format as described previously [33, 36]. Gels were incubated at 37°C for 4–6 days until use. Primary human umbilical vein endothelial cells (HUVEC) were prepared as described [36] and used without further passage. $2x10^4$ HUVEC were added to each collagen gel and incubated in Medium 199 (Life Technologies, Carlsbad, CA, USA) containing 20% human serum for 3 days to allow confluent monolayers to form. Media were prepared using a single batch of pooled human serum (pHS) prepared from six HIV-seronegative blood donors (Australian Red Cross Blood Service, Sydney, Australia) or autologous serum (from the same donor as the monocytes) as indicated; all sera were heat inactivated at 56°C for 30 min prior to use. Silver staining was performed on selected wells, in addition to routine phase-contrast microscopy, to verify HUVEC monolayer integrity (Supplementary Fig. 1A) [33]. HUVEC were activated with 10 ng/ml TNF for 4 hours [35] or left unactivated, then freshly isolated PBMCs ($2x10^5$/well) or purified monocytes ($5x10^4$/well) added for 1 hour at 37°C. Non-migrated cells were removed by washing and cultures incubated for a further 48 hours as described [33]. For TNF blocking, 10 or 20 μg/ml anti-TNFRI and anti-TNFRII (R&D Systems, Minneapolis, MN, USA), or respective isotype controls, were added immediately following monocyte

migration. Forty-eight hours after monocyte migration, reverse-migrated cells were removed and collagen gels stained with Oil Red O as described [35]. Gels were excised from wells, mounted on glass slides and foam cells counted by bright field microscopy (x40). Foam cells were defined as cells containing Oil Red O stained vesicles within the cytoplasm and determined as a proportion of total migrated cells within the counted area of the gel (Supplementary Fig. 1B). To investigate the phenotype of migrated cells within the collagen matrix, cells were extracted from the collagen by washing the gels without fixation and incubating in 1 mg/ml collagenase D for 20 min at 37°C, after which they were macerated manually and incubated further for 20 min at 37°C. Resulting cell suspensions were filtered through 100 μm mesh prior to staining for flow cytometric analysis. Cells extracted from collagen gels were stained with 0.2μg/mL BODIPY® 493/503 (Life Technologies, Carlsbad, CA, USA) in 150mM NaCl for 20 min at room temperature and anti-TNF-PE, CD36-FITC, CD14-APC and CD11b-PE (all from BD Biosciences, San Jose, CA) as described [20]. Cells stained with anti-CD14 APC and BODIPY were sorted using a BD influx cell sorter. The specificity of phenotyping antibodies was verified via the use of isotype control antibodies on selected samples (Supplementary Figure 2).

Live-cell imaging

Purified monocytes were stained with PKH26 (Sigma-Aldrich, St Louis, MO, USA) according to manufacturer's instructions and added to HUVEC monolayers grown on collagen gels in 96-well optical plates (Greiner Bio-One, Frickenhausen, Germany). Cells were immediately incubated at 37°C in a humidified temperature-controlled chamber coupled to a DeltaVision deconvolution microscope (Applied Precision-GE Healthcare, Issaquah, WA, USA) and images were captured in z-series on a CCD camera through a 20x 0.45 NA lens. Detection and tracking of cell migration was performed using the tracking module of the Imaris software (Bitplane, Zurich, Switzerland).

Analysis of plasma lipids and soluble factors

Plasma TNF and CXCL10 levels were measured using commercial ELISA kits (human TNF-α ELISA, Cardinal Bio-research, New Farm, Australia and Human CXCL10/IP-10 Quantikine ELISA KIT, R&D Systems, Minneapolis, MN, USA). Cholesterol and oxidized LDL levels in plasma were measured using the HDL and LDL/VLDL Cholesterol Assay Kit and the Human Oxidized LDL ELISA Kit (CML-LDL) respectively (both from Cell Biolabs, San Diego, CA, USA).

Cholesterol efflux assays

PBMCs (2.5–5 x 10^5) were incubated for 1 hour at 37°C in RPMI containing 10% pHS (RH-10) containing 1.5μM BODIPY-cholesterol (Avanti Polar Lipids, Alabaster, AL, USA), 6μM cholesterol and 300μM methyl-β-cyclodextrin (both from Sigma-Aldrich). Cells were washed twice with PBS- (PBS without Mg^{2+} or Ca^{2+}), resuspended in RH-10 and cholesterol was allowed to efflux from the cells for 30 min at 37°C in either the absence or presence of 1mM of methyl-β-cyclodextrin. Cells were washed, fixed with 1% formaldehyde, immuno-stained as above and analyzed by flow cytometry.

Gene expression analysis of cholesterol efflux and metabolism intermediates

The expression of proteins involved in cholesterol metabolism and transport was assessed via quantitative real-time PCR (qPCR). Monocytes were isolated from frozen PBMC, rested for 4 hours in RPMI containing 20% pHS at 37°C and total RNA was extracted. Potential DNA contamination was removed by DNase I treatment (37°C for 20 min, 75°C for 10 min, Roche, Basel, Switzerland). cDNA synthesis was performed using a combination (1:2) of oligo(dT) and random hexamer primers respectively (Transcriptor First Strand cDNA synthesis kit, Roche) and qPCR analysis was performed using FastStart Universal SYBR Green Master Mix (Roche) for GAPDH, ATP-binding cassette transporter A1 (ABCA1) and Acyl-coenzyme A: cholesterol acyltransferase (ACAT), and Brilliant SYBR II (Agilent Technologies, Santa Clara, CA, USA) for ABCG1 and HMG-CoA reductase on a MX3005P qRT-PCR machine (Agilent Technologies). The primers used were: GAPDH (Fwd 5′-CCATGGCACCGTCAAGGC-3′, Rev 5′-CCAGCATCGCCCCACTTG-3′), ABCA1 (Fwd 5′-GCACTGAGGAAGATGCTGAAA-3′, Rev 5′-AGTTCCTGGAAGGTCTTGTTCAC-3′), ABCG1 (Fwd 5′-CAGGAAGATTAGACACTGTGG-3′, Rev 5′-GAAAGGGGAATGGAGAGA-3′), ACAT (Fwd 5′-CAAGGCGCTCTCTCTTAGATGAAC-3, Rev 5′-GATAAAGAGAATGAGGAGGGCAATAA-3′) and HMG-CoA reductase (Fwd 5′-GGGACCAACCTACTACCTCAG-3′, Rev 5′-CGACCTGTTGTGAATCATGTGACTT-3′) at a final concentration of 280 nM of each primer. PCR conditions were 95°C for 10 min then 40 cycles of 95°C for 15 sec, 60°C for 1 min. Absolute quantification of gene expression was determined via comparison to a standard curve generated from serial dilution of a plasmid engineered to contain the amplicon of interest. Expression of all genes was standardized to GAPDH.

Data and statistical analysis

Non-parametric, two-tailed Mann-Whitney U test was used for unpaired data and Wilcoxon rank-sum test for paired data. Parametric unpaired t-test was used for data passing the D'Agostino-Pearson omnibus normality test. Statistical analysis was performed using GraphPad Prism software where values of $p<0.05$ were considered statistically significant.

RESULTS

HIV infection increases foam cell formation by monocytes following transendothelial migration

We have previously shown that HIV infection of monocyte-derived macrophages *in vitro* impairs their ability to reverse migrate across a HUVEC-collagen gel model of early atherosclerotic events [36], suggesting these cells may have a greater propensity to differentiate into foam cells and thus be retained in the collagen matrix. To investigate whether HIV infection *in vivo* is associated with increased propensity for monocytes to develop into foam cells, we utilized a refined version of this model to analyze the atherogenic properties of monocytes isolated by negative selection from fresh whole blood. Ageing is well documented to increase the risk of atherosclerosis, thus we investigated the effect of HIV infection in younger HIV+ individuals and uninfected controls of a similar age. Monocytes were isolated from seven healthy controls (all male, median age [range]

29.0 [25–56] years) and eight HIV+ males (median age 36.5 [26–47] years). Of the HIV+ individuals, four were receiving cART and had low (80 copies/ml, n=1) or undetectable (<40 copies/ml, n=3) viral loads and the remaining four were not receiving cART and had a median viral load of 23,400 copies/ml (range: 300 to 254,800 copies/ml).

When added to unstimulated HUVEC in media containing 20% pHS, a significantly increased proportion of monocytes from HIV+ individuals differentiated into foam cells as compared to monocytes from control subjects (median foam cells 18.9% vs 0%, respectively, p=0.004, Fig. 1A; all samples tested using the same batch of pHS). To determine whether factors present in HIV+ serum may further influence foam cell formation, we analyzed foam cell formation using culture media containing autologous serum rather than pHS and found that whilst foam cell formation by control monocytes was not significantly altered in the presence of autologous serum, serum from HIV+ individuals significantly increased foam cell formation by autologous monocytes (p=0.03, Fig. 1A).

Consistent with our previous findings, activation of HUVEC with TNF prior to monocyte migration significantly increased foam cell formation by monocytes from control donors (p=0.016 for both pHS and autologous serum, Fig. 1A vs B) and also HIV+ monocytes in the presence of pHS (p=0.008). As seen with unactivated HUVEC, autologous serum from HIV+ but not control individuals significantly increased foam cell formation when monocytes were added to TNF activated HUVEC (p=0.02 vs 0.30 respectively, Fig. 1B). The increased rate of foam cell formation by control monocytes following endothelial cell activation meant that differences between control and HIV+ monocytes were only observed in the presence of autologous serum (p=0.03, Fig. 1B). Similar levels of foam cell were formed by monocytes from young HIV+ individuals receiving cART with low/undetectable viral loads as compared to young untreated HIV+ individuals with viremia (Supplementary Fig. 3A and B). We also analyzed foam cell formation in an expanded cohort of 17 HIV+ males aged 26–68 years consisting of 13 individuals receiving cART (12 virologically suppressed with plasma viral loads <40 copies/ml and one individual with 80 copies/mL) plus the four viremic individuals not receiving cART defined above. This analysis showed a non-significant trend towards increased foam cell formation with age however there were no differences between virologically suppressed and non-suppressed HIV+ individuals (Supplementary Fig. 3C). Data from this expanded cohort of largely virologically suppressed individuals also confirmed the pro-atherogenic effect of autologous HIV+ serum (Supplementary Fig. 3D).

We then determined whether the pro-atherogenic effect of HIV+ serum was only evident in combination with autologous HIV+ monocytes or whether it was also capable of enhancing foam cell formation by monocytes from HIV-seronegative individuals. To investigate this, we analyzed foam cell formation in the model described above using monocytes from six HIV-uninfected controls in the presence of either pHS, or serum from five cART-treated, virologically suppressed HIV+ individuals. Foam cell formation by control monocytes was significantly increased by all five HIV+ sera used (Fig. 1C), confirming the presence of soluble factor(s) in HIV+ sera that promote foam cell formation. Significantly, the sera used in this experiment were all from patients with undetectable viral load, indicating the responsible factors remain elevated despite viral suppression. The above data indicate that

HIV infection promotes the differentiation of monocytes into foam cells via a mechanism involving both soluble factors present in the serum and an intrinsic alteration to monocyte function.

Live cell imaging of monocyte migration in the TEM assay

To investigate the effect of HIV infection on monocyte movement post-migration, we labeled monocytes with the fluorescent membrane dye PKH26, and recorded individual cell tracks within the collagen layer using live cell imaging over 48 hours (Fig. 2 and Fig 2mov1 and Fig 2mov2). Tracks obtained from monocytes from HIV+ subjects showed a greater number of slowly-migrating cells (indicated by yellow foci in Fig. 2B vs control donor in 2A), consistent with more monocytes developing into non-motile foam cells. This behavior was observed for monocytes from virologically suppressed HIV+ individuals receiving cART using either control serum or autologous serum (data not shown). We calculated the distribution of displacement length using tracks combined from at least three independent experiments and found that monocytes from HIV+ individuals migrated shorter distances than those from control subjects (evidenced by a shift to the left in the distance frequency histograms for HIV+ samples, Fig. 2C) and this effect was heightened in the presence of autologous HIV+ serum (Fig. 2C).

Whilst the initial migration speed of monocytes from HIV+ individuals was not different from control monocytes in the presence of pHS, the presence of autologous serum was associated with a significant increase in initial migration speed (Fig. 2D), suggesting factors in HIV+ sera accelerate monocyte migration at early time-points after transendothelial migration. In contrast, tracks from HIV+ donors during the later stages of observation (i.e. 38–48 hours) showed a lower migration speed as compared to control monocytes (Fig. 2E). Interestingly, the average migration speed of monocytes from HIV+ individuals was higher in the presence of autologous serum vs pHS, although the speed was still significantly lower than that of control monocytes (Fig. 2E). Analysis of monocyte speed over the entire observation window (0–48 hours) confirmed the overall average migration speed of monocytes from HIV+ individuals was lower than that of controls (not shown). These data indicate that monocytes from HIV+ individuals have impaired movement post-transendothelial migration, consistent with their differentiation into foam cells, and that factors present in the serum of HIV+ individuals enhance this effect.

Plasma TNF and CXCL10 levels are increased in HIV+ individuals

HIV infection is associated with dyslipidemia due to the combined effects of HIV and certain antiretroviral drugs, which may influence the atherogenic properties of monocytes and sera from HIV+ individuals. To determine whether altered cholesterol levels in autologous serum were responsible for the increase in foam cell formation by monocytes from HIV+ individuals in this study, we measured plasma levels of HDL, LDL and oxLDL by ELISA. No significant differences were observed in plasma levels of any of these forms of cholesterol between HIV+ and control individuals (Supplementary Fig. 4), suggesting that the heightened foam cell formation by HIV+ monocytes observed here is unlikely to be due solely to altered levels of these cholesterol species in the blood.

Inflammatory factors activate monocytes and can also drive foam cell formation independent of dyslipidemia (reviewed in [37]), therefore we measured plasma levels of the pro-inflammatory cytokine TNF and the monocyte activation biomarker CXCL10 in our cohort. Both CXCL10 and TNF levels were significantly elevated in HIV+ as compared to control individuals (Fig. 3A and B, p=0.01 and 0.03 respectively). Taken together, these data suggest that plasma markers of monocyte activation and inflammation, but not plasma cholesterol levels, are significantly increased in these HIV+ individuals who also show increased foam cell formation.

Anti-TNF receptor blocks foam cell formation independent of HUVEC activation

We have shown here and previously [35] that TNF activates endothelial cells to increase foam cell formation, and plasma TNF levels have been found to be elevated in HIV patients irrespective of cART [38]. We therefore considered whether TNF promotes foam cell differentiation independently of its effects on HUVEC. Monocytes from control donors were allowed to migrate through TNF-activated HUVEC, then blocking antibodies to TNF receptor (TNFR) I and II were added to media containing either control pHS or serum from virologically suppressed HIV+ donors and cells incubated for 48 hours. Monocytes from each control donor were incubated with serum from three different HIV+ donors, with serum from a total of six HIV+ donors utilized for these experiments. Anti TNFR antibodies reduced foam cell formation in a dose-dependent manner compared to cells treated with isotype control antibodies (Fig. 3C), and this inhibition was observed when either control serum (pHS) or HIV+ serum was used. These data suggest that endogenous TNF in serum, and/or TNF produced by activated monocytes during foam cell differentiation, enhances foam cell formation independently of its effects on endothelial activation, and that increased levels of TNF in individuals with HIV likely contributes to the pro-atherogenic effect of HIV + serum.

Foam cells down-regulate markers associated with immunity and endothelial attachment

To characterize the foam cells generated in our model following monocyte transendothelial migration, we labelled migrated cells extracted from the collagen with the fluorescent lipophilic dye BODIPY to enable detection of foam cells and macrophages via flow cytometry. To confirm the ability of BODIPY staining to identify foam cells, we analyzed labelled cells using imaging flow cytometry and found that cells with high BODIPY staining exhibited a morphology consistent with foam cells (Supplementary Fig. 5). By gating $BODIPY^{high}$ cells the percentage of foam cells was determined based on fluorescence intensity (rather than visually, which may be subjective). This gave similar values to those determined by Oil Red O staining and light microscopy analysis assayed in parallel (Supplementary Fig. 5). Taken together, these data confirm that both BODIPY and Oil Red O staining were able to identify similar populations of foam cells and macrophages within our model.

Having validated the use of fluorescent BODIPY staining for identification of foam cells, we labelled cells extracted from the collagen matrix with both anti-CD14 and BODIPY and analyzed them by standard flow cytometry. This revealed two distinct populations of CD14+ cells; large, $BODIPY^{high}CD14^{low}$ cells with high granularity, consistent with foam cells, and

a population of smaller BODIPY^{low}CD14^{high} cells with relatively low granularity, consistent with monocytes/immature macrophages (Fig. 4A). The characterization of these two novel populations was confirmed by microscopic analysis of FACS sorted cells and was consistent in experiments using monocytes from 14 independent donors (Fig. 4B–C).

We further analyzed the phenotype of macrophages and foam cells by measuring expression of the β_2 integrin subunit CD11b and the oxLDL receptor CD36. Foam cells had lower expression of both receptors compared to macrophages, consistent with a role in lipid storage as opposed to migration and active lipid accumulation (Fig. 4D–E). Moreover, foam cells had significantly higher intracellular levels of TNF compared to macrophages (Fig. 4F), indicating a pro-inflammatory phenotype. These observations show that foam cell formation is associated with increased cell size, reduced surface expression of CD14, CD11b and CD36 but an increase in the production of the pro-inflammatory cytokine TNF.

Monocytes from HIV+ individuals showed impaired cholesterol efflux and reduced expression of cholesterol transporters

The above data indicate that monocytes from HIV+ individuals have an increased potential to form foam cells, independent of the atherogenic effects of serum, suggesting that HIV is associated with intrinsic changes to monocytes that may alter lipid transport. We therefore assessed the ability of monocytes from virologically suppressed cART-treated individuals to efflux cholesterol using an *ex vivo* assay. PBMC from HIV+ individuals and controls of a similar age (n=8 each, all male, median age (range) 43.5 (33–51) and 36.5 (28–52) respectively) were loaded with BODIPY-labelled cholesterol and the subsequent cholesterol efflux from monocytes determined via flow cytometry. This analysis revealed that monocytes from HIV+ individuals were significantly impaired in their ability to efflux cholesterol from the cell, and this impairment was evident both in the absence and presence of the exogenous cholesterol scavenger methyl-β-cyclodextrin (Fig. 5A and B respectively).

To investigate the mechanistic basis for this impairment, we analyzed the expression of key genes involved in cholesterol synthesis and transport. RNA was extracted from monocytes purified from virologically-suppressed HIV+ individuals on cART and age-matched controls and gene expression analyzed via qPCR. This analysis revealed significantly reduced expression of the key cholesterol efflux transporter ABCA1 in monocytes from HIV+ individuals (Fig. 5C, p=0.02), whilst expression of ABCG1 showed a similar although not statistically significant down-regulation (Fig. 5D). Expression of HMG-CoA reductase, the rate-determining enzyme for cholesterol biosynthesis, was also significantly reduced in monocytes from individuals with HIV (Fig. 5E, p=0.02), whilst monocyte expression of the cholesterol esterase ACAT was not altered by HIV infection (Fig. 5F). These data indicate that HIV infection is associated with a decreased expression of key cholesterol efflux genes in monocytes and an impaired ability to efflux cholesterol from the cell, which likely contributes to the increased potential of monocytes from HIV+ individuals to form foam cells.

DISCUSSION

Using a model of atherosclerosis that couples primary human monocyte transendothelial migration and foam cell differentiation, we show that monocytes from HIV+ individuals have a higher rate of foam cell formation, which is due to both intrinsic changes to monocyte function and a pro-atherogenic effect of soluble factors present in HIV+ serum. These findings may provide some of the first mechanistic evidence regarding the pathogenesis of increased atherosclerosis and CVD in the setting of HIV infection.

In this study, we adapted our *in vitro* model which couples monocyte transendothelial migration and foam cell formation to determine the functional properties of human monocytes purified from an HIV+ patient cohort. The strengths of this model include a) monocytes migrate through an activated primary human endothelial monolayer in response to chemokines secreted *in situ* and into a fibrous collagen matrix that mimics the subendothelial neointima, b) it measures foam cell formation by migrated monocytes, rather than *in vitro* differentiated macrophages and c) exogenous modified lipoprotein is not added, therefore foam cells form in response to endogenous lipids in the human-serum containing media and/or generated in response to endothelial activation. This model is therefore a physiologically relevant system for studying the early stages of foam cell formation *in vitro* by migrating human monocytes.

Although HIV infection and certain antiretroviral drugs including protease inhibitors can cause dyslipidemia [39], plasma levels of LDL, HDL and oxLDL in the HIV+ individuals who contributed to this study were not different from controls, suggesting that heightened foam cell formation observed here cannot be explained by lipidemic HIV+ serum alone. Endothelial activation and/or monocyte transendothelial migration may affect levels of oxLDL within the gels however, which could influence foam cell formation. Significantly, serum from HIV+ individuals had elevated levels of TNF and foam cell formation was blocked by anti-TNF receptor antibodies added after monocyte migration, supporting a pro-atherogenic role for TNF in these individuals via mediating monocyte activation and increased foam cell formation. Our data were qualitatively supported by live-cell imaging showing monocytes from HIV+ individuals moved more slowly within the collagen matrix of the model, particularly at later times, consistent with differentiation into foam cells. These novel data regarding the pro-atherogenic properties of monocytes from HIV+ individuals may provide a mechanistic explanation for increased atherosclerosis in this population.

In addition to the pro-atherogenic effects of HIV+ serum, our data suggest HIV infection induces changes to monocytes that predispose them to foam cell formation. Indeed, we found an altered expression of critical cholesterol synthesis and transport proteins in monocytes from HIV+ individuals. The reduced gene expression of ABCA1 may translate to an impaired ability to remove cholesterol from the cell, consistent with our observation of impaired cholesterol efflux in monocytes from individuals with HIV. Feeney *et al* also examined the expression of cholesterol metabolism genes in monocytes and found reduced levels of ABCA1 mRNA in viremic but not virologically-suppressed HIV+ participants, whilst expression of the lipid uptake receptors CD36 and LDL-receptor was reduced in both HIV+ groups [40]. The different result regarding ABCA1 expression may be due to

differences in the methodology of monocyte isolation (positive selection in the Feeney *et al* study as compared to negative selection used in our study), differences in the cohorts used (50% female and 64% non-white vs 100% white males in our study) or the smaller sample size in our study. Thus, these findings need to be confirmed in a larger cohort adequately powered to examine the effect of demographic factors including sex and race. The reduced expression of the cholesterol synthesis enzyme HMG-CoA reductase in monocytes shown here is consistent with the previously reported study and may represent a cellular response to increased intracellular cholesterol levels.

The foam cell data presented here were generated from a combination of virologically-suppressed and non-suppressed individuals. Although analysis of foam cell formation in an expanded HIV+ cohort aged 26–68 years did not reveal any significant differences associated with detectable levels of viremia this requires confirmation in a larger sample set. The fact that serum from virologically-suppressed individuals enhanced foam cell formation suggests the persistence of pro-atherogenic factors in serum in individuals receiving effective cART. Furthermore, our findings of impaired cholesterol efflux from monocytes were also made in virologically-suppressed individuals, consistent with our findings that increased monocyte and innate immune activation associated with HIV infection are maintained following viral suppression by cART [20, 21]. It remains possible that antiretroviral agents may contribute to this phenotype in cART-treated individuals, however this requires investigation. Given only a very small proportion of monocytes are found to be infected with HIV *in vivo* (<0.1%), the proatherogenic monocyte phenotype observed here is likely secondary to HIV-associated immune activation and inflammation and not a result of direct infection, although it remains possible that non-productive/latent HIV infection may also alter monocyte phenotype. Our data suggest monocytes from virologically-suppressed individuals receiving cART exhibit a pro-atherogenic activity and that this may be a pathogenic factor underlying increased atherosclerotic risk in HIV+ individuals.

Endothelial activation plays an integral role in atherosclerosis and monocyte transendothelial migration via the expression of adhesion molecules (reviewed in [41]), and soluble endothelial activation markers are elevated in HIV+ individuals and independently associated with carotid intima-media thickness, a surrogate measure of atherosclerosis [42]. Zietz *et al* examined the aortic endothelium of patients largely with advanced HIV disease and found structural abnormalities which were accompanied by increased expression of adhesion molecules and mononuclear cell infiltration [43]. Thus, the proatherogenic effects of HIV+ monocytes observed here may well be potentiated by heightened endothelial cell activation *in vivo*. Pro-inflammatory cytokines are well documented to be associated with increased cardiovascular risk factors and outcomes in both HIV+ and seronegative individuals (reviewed in [44]), however viral factors in the blood may also contribute to increased atherosclerosis in HIV infection. HIV infection and HIV-derived single stranded RNAs increase foam cell formation by monocyte-derived macrophages *in vitro* [45, 46]. The HIV accessory protein Nef promotes foam cell formation in these cells by inhibiting cholesterol efflux [45], and high concentrations of Nef persist in plasma of HIV+ individuals receiving cART [47]. Taken together, it is therefore likely that changes to both monocyte activation and gene expression together with inflammatory cytokines and virus-specific factors in serum contribute to the pro-atherogenic potential of monocytes observed here.

Heightened foam cell formation by monocytes/macrophages *in vitro* is consistent with increased prevalence of atherosclerotic plaques in HIV+ as compared to uninfected individuals [4, 22, 48], and it would be of interest to determine whether this is associated with altered plaque morphology in HIV+ individuals *in vivo*.

We devised a technique to differentiate between monocyte-derived macrophages and monocyte-derived foam cells produced in our model based on CD14 and BODIPY staining and determined that foam cells have an inflammatory phenotype, as defined by higher TNF and down-regulated CD11b expression similar to that described by others [49]. Higher intracellular TNF levels compared to migrated macrophages suggests foam cells may have a positive feedback role in activating the endothelium and promoting oxidation of LDL during the development of atherosclerotic plaques, as well acting on nearby foam cells to enhance cellular activation. We also found foam cells down-regulated expression of CD14, CD11b and CD36, the latter two being critical for monocyte attachment and lipid uptake, respectively. Down-regulation of CD36 expression was unexpected as CD36 contributes to foam cell formation [35]. Whilst reduced CD36 expression in response to uptake of modified LDL particles has been reported by others [50], the majority of studies suggest oxLDL particles increase CD36 expression [51, 52] and CD36 is highly expressed in foam cells obtained from mature human plaques [53]. The kinetics of CD36 expression during the process of foam cell formation is poorly understood, and the decreased CD36 expression we observed may be the result of receptor internalization due to endocytosis of lipid, or may be a transient response to lipid uptake immediately after migration. Indeed, our model analyses foam cells formed within 48 hours of migration, whereas foam cells extracted from human plaques likely developed over longer periods. This, combined with findings from parallel studies indicating that foam cells extracted from our model are smaller and contain less cholesterol ester than mature foam cells extracted from atherosclerotic plaques (unpublished findings), suggests they likely represent immature foam cells or foam cell precursors. Studying the behavior of these cells is therefore highly relevant for strategies aimed at preventing or reversing the early stages of foam cell formation.

Our study reports novel data indicating that monocytes from HIV+ individuals, a population characterized by chronic inflammation and immune activation, have a greater propensity to differentiate into foam cells and that elevated levels of TNF in plasma of these individuals further enhances this effect. This may explain the increased risk of atherosclerosis in these individuals after adjusting for viral and traditional risk factors and warrants further clinical investigation of the relationship between monocyte activation, atherogenic behavior and the development of atherosclerosis in HIV+ individuals receiving cART.

Supplementary Material

Refer to Web version on PubMed Central for supplementary material.

Acknowledgments

We wish to thank The Alfred hospital Infectious Disease Unit staff for patient recruitment, Dr Clare Westhorpe for technical expertise and training, Maelenn Gouillou for assistance with statistical analysis, Dr Bill Kalionis and research nurses at the Royal Women's Hospital, Melbourne and Nguyen Thanh Thao Le for help with cord

collection and HUVEC preparation respectively, the AMREP Flow Cytometry Core and Burnet Cell Imaging Facilities, Dr Annie Yan and Ben Hibbs from the Melbourne Materials Institute, Melbourne University for assistance with imaging flow cytometry and all participants who generously donated blood for this project.

Sources of funding

The authors gratefully acknowledge the contribution to this work of the Victorian Operational Infrastructure Support Program received by the Burnet Institute. AM is supported by the Postdoctoral Programme of the German Academic Exchange Service (DAAD) and an Occupational Trainee Scholarship of the Burnet Institute. SC is a recipient of a National Health and Medical Research Council of Australia (NHMRC) Principal Research Fellowship. WAM is supported by grants R01 HL046849 and R37 HL064774 from the NIH. The work was funded via NHMRC project grants to AJ.

References

1. Marin B, Thiebaut R, Bucher HC, Rondeau V, Costagliola D, Dorrucci M, et al. Non-AIDS-defining deaths and immunodeficiency in the era of combination antiretroviral therapy. AIDS. 2009; 23(13): 1743–53. [PubMed: 19571723]
2. Rodger AJ, Lodwick R, Schechter M, Deeks S, Amin J, Gilson R, et al. Mortality in well controlled HIV in the continuous antiretroviral therapy arms of the SMART and ESPRIT trials compared with the general population. AIDS. 2013; 27(6):973–9. [PubMed: 23698063]
3. Hsue PY, Hunt PW, Schnell A, Kalapus SC, Hoh R, Ganz P, et al. Role of viral replication, antiretroviral therapy, and immunodeficiency in HIV-associated atherosclerosis. AIDS. 2009; 23(9): 1059–67. [PubMed: 19390417]
4. Lo J, Abbara S, Shturman L, Soni A, Wei J, Rocha-Filho JA, et al. Increased prevalence of subclinical coronary atherosclerosis detected by coronary computed tomography angiography in HIV-infected men. AIDS. 2010; 24(2):243–53. [PubMed: 19996940]
5. Currier JS, Taylor A, Boyd F, Dezii CM, Kawabata H, Burtcel B, et al. Coronary heart disease in HIV-infected individuals. J Acquir Immune Defic Syndr. 2003; 33(4):506–12. [PubMed: 12869840]
6. Obel N, Thomsen HF, Kronborg G, Larsen CS, Hildebrandt PR, Sorensen HT, et al. Ischemic heart disease in HIV-infected and HIV-uninfected individuals: a population-based cohort study. Clin Infect Dis. 2007; 44(12):1625–31. [PubMed: 17516408]
7. Triant VA, Lee H, Hadigan C, Grinspoon SK. Increased acute myocardial infarction rates and cardiovascular risk factors among patients with human immunodeficiency virus disease. J Clin Endocrinol Metab. 2007; 92(7):2506–12. [PubMed: 17456578]
8. Freiberg MS, Chang CC, Kuller LH, Skanderson M, Lowy E, Kraemer KL, et al. HIV infection and the risk of acute myocardial infarction. JAMA Intern Med. 2013; 173(8):614–22. [PubMed: 23459863]
9. Hsue PY, Lo JC, Franklin A, Bolger AF, Martin JN, Deeks SG, et al. Progression of atherosclerosis as assessed by carotid intima-media thickness in patients with HIV infection. Circulation. 2004; 109(13):1603–8. [PubMed: 15023877]
10. Lorenz MW, Stephan C, Harmjanz A, Staszewski S, Buehler A, Bickel M, et al. Both long-term HIV infection and highly active antiretroviral therapy are independent risk factors for early carotid atherosclerosis. Atherosclerosis. 2008; 196(2):720–6. [PubMed: 17275008]
11. Parra S, Coll B, Aragones G, Marsillach J, Beltran R, Rull A, et al. Nonconcordance between subclinical atherosclerosis and the calculated Framingham risk score in HIV-infected patients: relationships with serum markers of oxidation and inflammation. HIV Med. 2010; 11(4):225–31. [PubMed: 19845792]
12. Friis-Moller N, Sabin CA, Weber R, d'Arminio Monforte A, El-Sadr WM, Reiss P, et al. Combination antiretroviral therapy and the risk of myocardial infarction. N Engl J Med. 2003; 349(21):1993–2003. [PubMed: 14627784]
13. Islam FM, Wu J, Jansson J, Wilson DP. Relative risk of cardiovascular disease among people living with HIV: a systematic review and meta-analysis. HIV Medicine. 2012; 13(8):453–468. [PubMed: 22413967]

14. Currier JS, Lundgren JD, Carr A, Klein D, Sabin CA, Sax PE, et al. Epidemiological evidence for cardiovascular disease in HIV-infected patients and relationship to highly active antiretroviral therapy. Circulation. 2008; 118(2):e29–35. [PubMed: 18566319]
15. El-Sadr WM, Lundgren J, Neaton JD, Gordin F, Abrams D, Arduino RC, et al. CD4+ count-guided interruption of antiretroviral treatment. N Engl J Med. 2006; 355(22):2283–96. [PubMed: 17135583]
16. Pereyra F, Lo J, Triant VA, Wei J, Buzon MJ, Fitch KV, et al. Increased coronary atherosclerosis and immune activation in HIV-1 elite controllers. AIDS. 2012; 26(18):2409–12. [PubMed: 23032411]
17. Hsue PY, Scherzer R, Hunt PW, Schnell A, Bolger AF, Kalapus SC, et al. Carotid Intima-Media Thickness Progression in HIV-Infected Adults Occurs Preferentially at the Carotid Bifurcation and Is Predicted by Inflammation. J Am Heart Assoc. 2012; 1(2)
18. Duprez DA, Neuhaus J, Kuller LH, Tracy R, Belloso W, De Wit S, et al. Inflammation, coagulation and cardiovascular disease in HIV-infected individuals. PLoS One. 2012; 7(9):e44454. [PubMed: 22970224]
19. De Luca A, de Gaetano Donati K, Colafigli M, Cozzi-Lepri A, De Curtis A, Gori A, et al. The association of high-sensitivity c-reactive protein and other biomarkers with cardiovascular disease in patients treated for HIV: a nested case--control study. BMC Infect Dis. 2013; 13(1):414. [PubMed: 24004495]
20. Hearps AC, Maisa A, Cheng WJ, Angelovich TA, Lichtfuss GF, Palmer CS, et al. HIV infection induces age-related changes to monocytes and innate immune activation in young men that persist despite combination antiretroviral therapy. AIDS. 2012; 26(7):843–53. [PubMed: 22313961]
21. Martin GE, Gouillou M, Hearps AC, Angelovich TA, Cheng AC, Lynch F, et al. Age-associated changes in monocyte and innate immune activation markers occur more rapidly in HIV infected women. PLoS One. 2013; 8(1):e55279. [PubMed: 23365694]
22. Burdo TH, Lo J, Abbara S, Wei J, Delelys ME, Preffer F, et al. Soluble CD163, a Novel Marker of Activated Macrophages, Is Elevated and Associated With Noncalcified Coronary Plaque in HIV-Infected Patients. J Infect Dis. 2011; 204(8):1227–36. [PubMed: 21917896]
23. Subramanian S, Tawakol A, Burdo TH, Abbara S, Wei J, Vijayakumar J, et al. Arterial inflammation in patients with HIV. JAMA. 2012; 308(4):379–86. [PubMed: 22820791]
24. Kelesidis T, Kendall MA, Yang OO, Hodis HN, Currier JS. Biomarkers of microbial translocation and macrophage activation: association with progression of subclinical atherosclerosis in HIV-1 infection. J Infect Dis. 2012; 206(10):1558–67. [PubMed: 23066162]
25. Westhorpe CL, Maisa A, Spelman T, Hoy JF, Dewar EM, Karapanagiotidis S, et al. Associations between blood monocyte markers and carotid atherosclerosis in HIV-positive patients. Immunol Cell Biol. 2014; 92(2):133–8. [PubMed: 24296810]
26. Baker JV, Hullsiek KH, Singh A, Wilson E, Henry K, Lichtenstein K, et al. Immunologic predictors of coronary artery calcium progression in a contemporary HIV cohort. AIDS. 2014; 28(6):831–40. [PubMed: 24370480]
27. Funderburg NT, Zidar DA, Shive C, Lioi A, Mudd J, Musselwhite LW, et al. Shared monocyte subset phenotypes in HIV-1 infection and in uninfected subjects with acute coronary syndrome. Blood. 2012; 120(23):4599–4608. [PubMed: 23065151]
28. Lusis AJ. Atherosclerosis. Nature. 2000; 407(6801):233–41. [PubMed: 11001066]
29. Febbraio M, Silverstein RL. CD36: implications in cardiovascular disease. Int J Biochem Cell Biol. 2007; 39(11):2012–30. [PubMed: 17466567]
30. Park YM, Febbraio M, Silverstein RL. CD36 modulates migration of mouse and human macrophages in response to oxidized LDL and may contribute to macrophage trapping in the arterial intima. J Clin Invest. 2009; 119(1):136–45. [PubMed: 19065049]
31. Galkina E, Ley K. Immune and inflammatory mechanisms of atherosclerosis (*). Annu Rev Immunol. 2009; 27:165–97. [PubMed: 19302038]
32. Llodra J, Angeli V, Liu J, Trogan E, Fisher EA, Randolph GJ. Emigration of monocyte-derived cells from atherosclerotic lesions characterizes regressive, but not progressive, plaques. Proc Natl Acad Sci U S A. 2004; 101(32):11779–84. [PubMed: 15280540]

33. Muller WA, Weigl SA. Monocyte-selective transendothelial migration: dissection of the binding and transmigration phases by an in vitro assay. J Exp Med. 1992; 176(3):819–28. [PubMed: 1512545]
34. Randolph GJ, Furie MB. A soluble gradient of endogenous monocyte chemoattractant protein-1 promotes the transendothelial migration of monocytes in vitro. J Immunol. 1995; 155(7):3610–8. [PubMed: 7561060]
35. Westhorpe CLV, Dufour EM, Maisa A, Jaworowski A, Crowe SM, Muller WA. Endothelial cell activation promotes foam cell formation by monocytes following transendothelial migration in an in vitro model. Exp Mol Pathol. 2012; 93(2):220–226. [PubMed: 22609311]
36. Westhorpe CL, Zhou J, Webster NL, Kalionis B, Lewin SR, Jaworowski A, et al. Effects of HIV-1 infection in vitro on transendothelial migration by monocytes and monocyte-derived macrophages. J Leukoc Biol. 2009; 85(6):1027–35. [PubMed: 19286896]
37. Angelovich TA, Hearps AC, Jaworowski A. Inflammation-induced foam cell formation in chronic inflammatory disease. Immunol Cell Biol. 2015; doi: 10.1038/icb.2015.26
38. Cassol E, Malfeld S, Mahasha P, van der Merwe S, Cassol S, Seebregts C, et al. Persistent microbial translocation and immune activation in HIV-1-infected South Africans receiving combination antiretroviral therapy. J Infect Dis. 2010; 202(5):723–33. [PubMed: 20629534]
39. Souza SJ, Luzia LA, Santos SS, Rondo PH. Lipid profile of HIV-infected patients in relation to antiretroviral therapy: a review. Rev Assoc Med Bras. 2013; 59(2):186–98. [PubMed: 23582562]
40. Feeney ER, McAuley N, O'Halloran JA, Rock C, Low J, Satchell CS, et al. The expression of cholesterol metabolism genes in monocytes from HIV-infected subjects suggests intracellular cholesterol accumulation. J Infect Dis. 2013; 207(4):628–37. [PubMed: 23204179]
41. Maslin CL, Kedzierska K, Webster NL, Muller WA, Crowe SM. Transendothelial migration of monocytes: the underlying molecular mechanisms and consequences of HIV-1 infection. Curr HIV Res. 2005; 3(4):303–17. [PubMed: 16250878]
42. Ross AC, Rizk N, O'Riordan MA, Dogra V, El-Bejjani D, Storer N, et al. Relationship between inflammatory markers, endothelial activation markers, and carotid intima-media thickness in HIV-infected patients receiving antiretroviral therapy. Clin Infect Dis. 2009; 49(7):1119–27. [PubMed: 19712036]
43. Zietz C, Hotz B, Sturzl M, Rauch E, Penning R, Lohrs U. Aortic endothelium in HIV-1 infection: chronic injury, activation, and increased leukocyte adherence. Am J Pathol. 1996; 149(6):1887–98. [PubMed: 8952525]
44. Hearps AC, Martin GE, Rajasuriar R, Crowe SM. Inflammatory Co-morbidities in HIV+ Individuals: Learning Lessons from Healthy Ageing. Curr HIV/AIDS Rep. 2014; 11(1):20–34. [PubMed: 24414166]
45. Mujawar Z, Rose H, Morrow MP, Pushkarsky T, Dubrovsky L, Mukhamedova N, et al. Human immunodeficiency virus impairs reverse cholesterol transport from macrophages. PLoS Biol. 2006; 4(11):e365. [PubMed: 17076584]
46. Bernard MA, Han X, Inderbitzin S, Agbim I, Zhao H, Koziel H, et al. HIV-derived ssRNA binds to TLR8 to induce inflammation-driven macrophage foam cell formation. PLoS One. 2014; 9(8):e104039. [PubMed: 25090652]
47. Raymond AD, Campbell-Sims TC, Khan M, Lang M, Huang MB, Bond VC, et al. HIV Type 1 Nef is released from infected cells in CD45(+) microvesicles and is present in the plasma of HIV-infected individuals. AIDS Res Hum Retroviruses. 2011; 27(2):167–78. [PubMed: 20964480]
48. Fitch KV, Srinivasa S, Abbara S, Burdo TH, Williams KC, Eneh P, et al. Noncalcified Coronary Atherosclerotic Plaque and Immune Activation in HIV-infected Women. J Infect Dis. 2013; 208(11):1737–46. [PubMed: 24041790]
49. Maiguel D, Faridi MH, Wei C, Kuwano Y, Balla KM, Hernandez D, et al. Small molecule-mediated activation of the integrin CD11b/CD18 reduces inflammatory disease. Sci Signal. 2011; 4(189):ra57. [PubMed: 21900205]
50. Kapinsky M, Torzewski M, Buchler C, Duong CQ, Rothe G, Schmitz G. Enzymatically degraded LDL preferentially binds to CD14(high) CD16(+) monocytes and induces foam cell formation mediated only in part by the class B scavenger-receptor CD36. Arterioscler Thromb Vasc Biol. 2001; 21(6):1004–10. [PubMed: 11397711]

51. Feng J, Han J, Pearce SF, Silverstein RL, Gotto AM Jr, Hajjar DP, et al. Induction of CD36 expression by oxidized LDL and IL-4 by a common signaling pathway dependent on protein kinase C and PPAR-gamma. J Lipid Res. 2000; 41(5):688–96. [PubMed: 10787429]

52. Hirano K, Yamashita S, Nakagawa Y, Ohya T, Matsuura F, Tsukamoto K, et al. Expression of human scavenger receptor class B type I in cultured human monocyte-derived macrophages and atherosclerotic lesions. Circ Res. 1999; 85(1):108–16. [PubMed: 10400916]

53. Nakata A, Nakagawa Y, Nishida M, Nozaki S, Miyagawa J, Nakagawa T, et al. CD36, a novel receptor for oxidized low-density lipoproteins, is highly expressed on lipid-laden macrophages in human atherosclerotic aorta. Arterioscler Thromb Vasc Biol. 1999; 19(5):1333–9. [PubMed: 10323787]

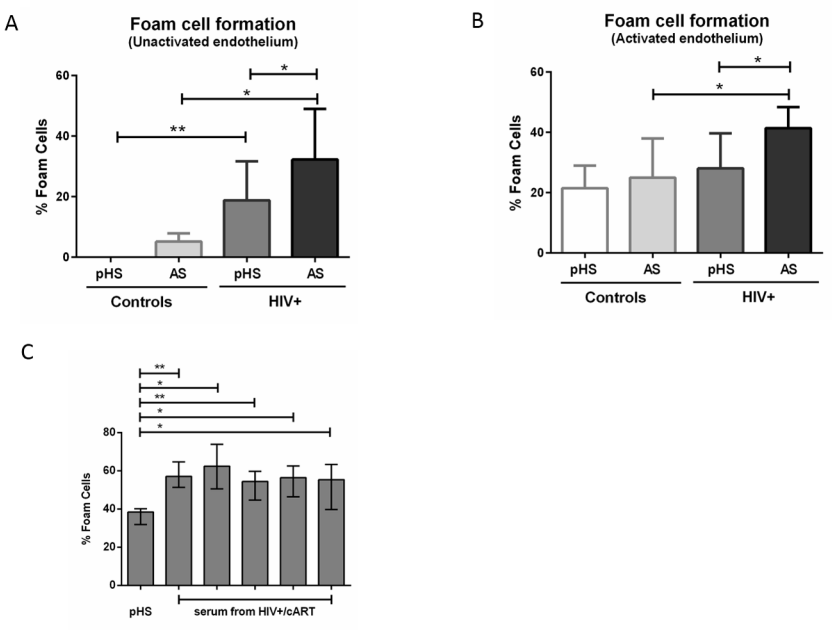

Figure 1. Monocytes from HIV+ subjects show increased foam cell formation which is enhanced by HIV+ serum

Percentage of foam cells present within collagen were measured following Oil Red O staining, as described in Methods, 48 hours after monocyte migration for seven HIV− controls and eight HIV+ male donors using (**A)** non-activated and (**B)** TNF-activated endothelium (HUVEC) in the presence of either pooled human control serum (pHS – identical batch used for all samples) or autologous serum (AS) from each individual donor. Bars represent median and interquartile range of data collected from 11 independent experiments. (**C)** Percentage of foam cells present within collagen was measured using monocytes prepared from six different HIV-negative donors added to TNF-activated HUVEC, and incubated with either pHS or serum from five different HIV+ donors receiving cART and with viral load <20 copies/ml. Box and whisker plots show median, IQR and 1.5xIQR (Tukey method). Paired two-tailed Wilcoxon rank sum test was used for within group comparisons and unpaired two-tailed Mann Whitney U test for between group comparisons. *p<0.05, **p<0.01.

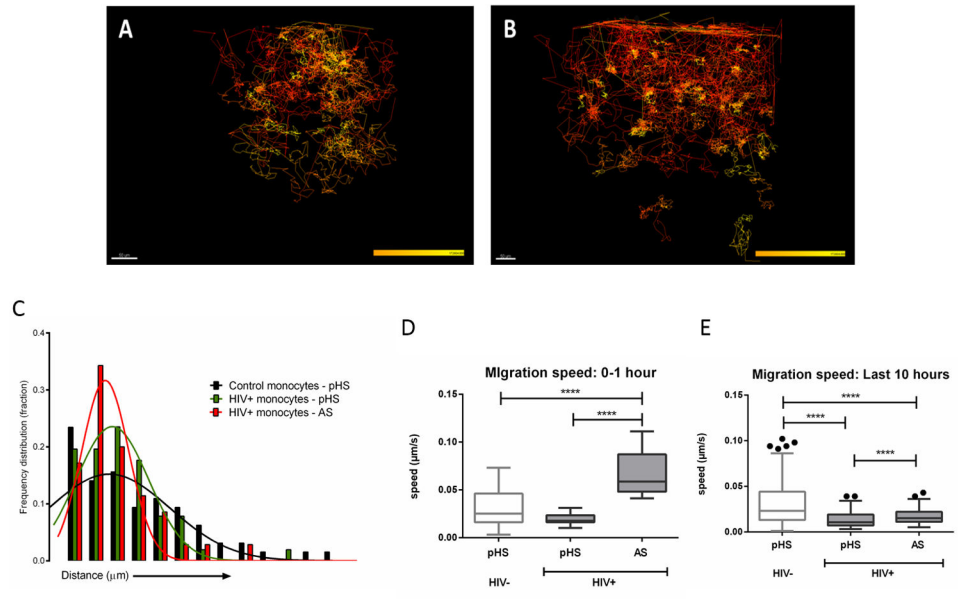

Figure 2. Tracking of monocyte migration via live cell imaging

Images were obtained from a representative experiment measuring migration over 48 hours of PKH26-labeled monocytes from a control donor (**A**) and HIV+ donor (**B**) in the presence of pooled human serum.. Cells were incubated at 37°C in a humidified temperature controlled chamber coupled to a DeltaVision microscope, images were captured using a CCD camera through a 20x 0.45 NA lens and cell movement was tracked over 48 hours. The color gradients represent time with red as the earliest time (closest to 0 hours) and yellow as latest time (closest to 48 hours; see also Fig 2mov1 and Fig 2mov2). (**C)** Tracks from live cell imaging experiments that could be assigned unambiguously to individual cells were identified and their displacement lengths computed using Imaris software. Frequency histogram of migration track lengths for monocytes added to unactivated HUVEC from HIV − controls in the presence of pooled human serum (pHS) (ctrl; black bars, 64 tracks combined from four independent experiments) or monocytes from HIV+ donors in the presence of pHS (green bars, 51 tracks/3 experiments) or autologous serum (AS; red bars, 35 tracks/3 experiments). Histograms are nudged by 10 data points. Average monocyte migration speed recorded in the first hour **(D)** or last 10 hours (**E**; hours 38–48) of migration for monocytes from HIV− controls in the presence of pHS and HIV+ donors in the presence of pHS or AS was computed using Imaris software. Box and whisker plots show median, IQR and 1.5xIQR (Tukey method; dots represent points outside these ranges). Significance was tested using an unpaired two-tailed Mann Whitney U test, **** $p<0.0001$.

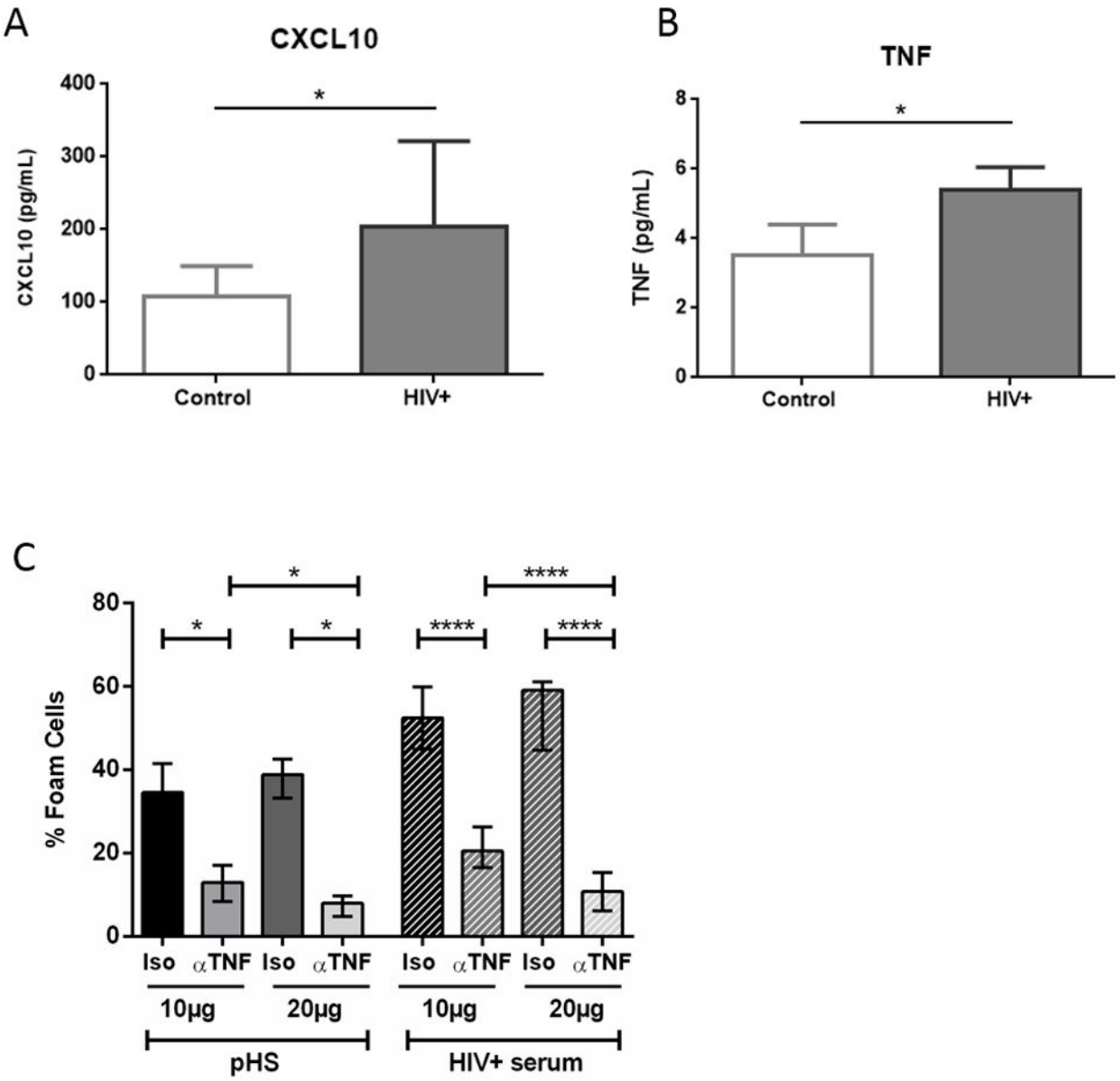

Figure 3. CXCL10 and TNF are elevated in HIV+ individuals and TNF acts at a post-migration stage to enhance foam cell formation

Concentration of **(A)** CXCL10 and **(B)** TNF in plasma from all subjects used in Figure 1 was measured by ELISA. Bars indicate median and interquartile range. * $p<0.05$, as determined by Mann-Whitney U test. **(C)** Percentage of foam cells within collagen gels was measured 48 hours after adding monocytes to TNF-activated HUVEC in the presence of the indicated amounts of antibodies to TNF receptors I and II (α-TNF), or isotype control (Iso) antibodies. Data are from monocytes isolated from six HIV-negative individuals incubated with pooled human serum (pHS) (left columns, n=6) or serum from virologically suppressed HIV+ donors (right, hatched columns; monocytes from each donor incubated with three different HIV+ sera, n=18). Differences between isotype and α-TNF treated samples were

detected using paired non-parametric two-tailed Wilcoxon rank sum test and between group differences detected using unpaired non-parametric two-tailed Mann Whitney U test, *p<0.05, ****p<0.0001.

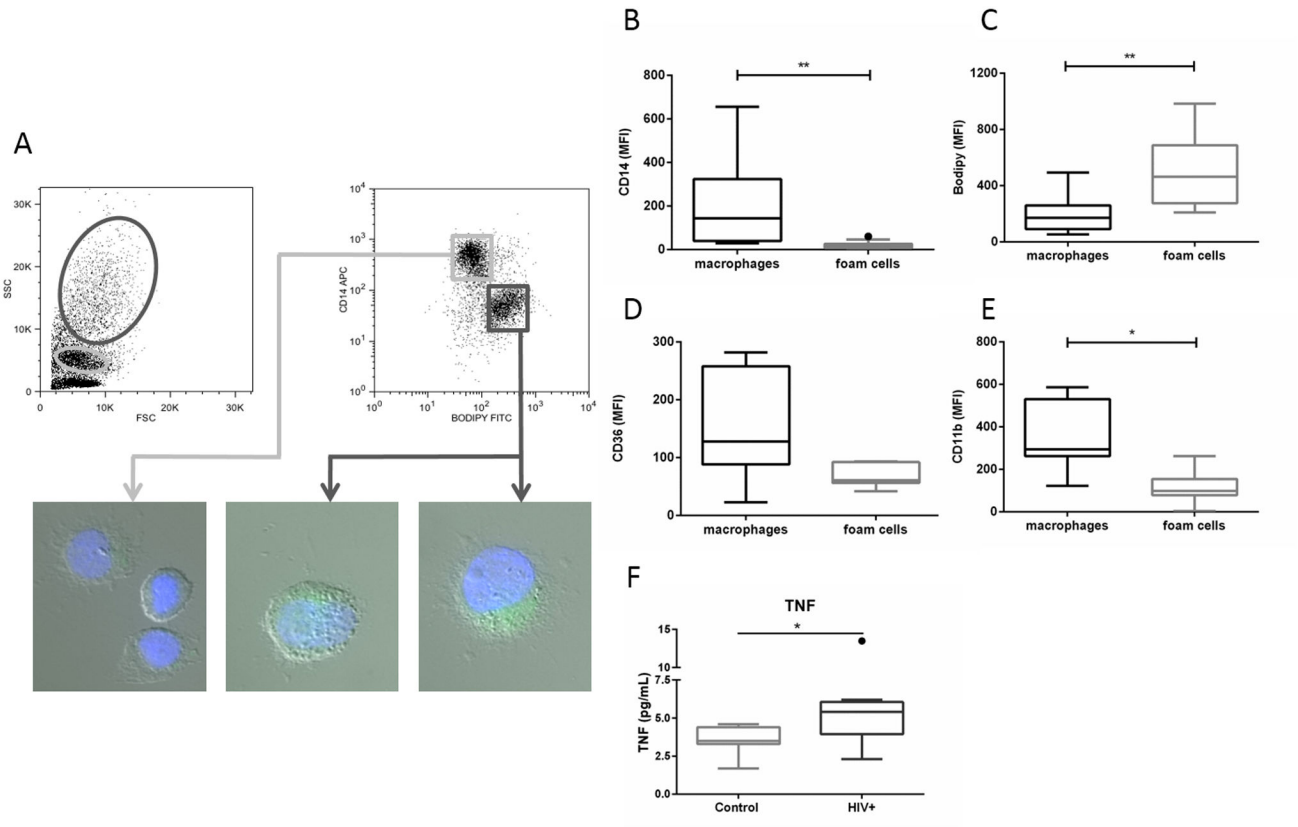

Figure 4. Flow cytometry analysis and sorting of transmigrated monocytes extracted from collagen gels

(A) Upper panels: Monocytes from a representative HIV− donor were extracted from collagen gels 48 hours after transmigration, stained with BODIPY 493/503 and anti-CD14-APC, then analyzed by flow cytometry. Left panel: FSC vs. SSC plot; Right panel: CD14-APC vs. BODIPY-FITC scatter plot. The two indicated populations were isolated by cell sorting. **Bottom panel:** FACS-purified cells from the gates shown were counterstained with Hoechst 33258, centrifuged onto glass slides and mounted in Fluoromount-G. Images were captured on a charge-coupled device (CCD) camera (AxioCamMRm Rev. 3, Carl Zeiss, Germany) through a 100x 1.3 numerical aperture oil immersion lens on a Zeiss Axio Observer.Z1 inverted microscope. **(B–F).** Cells extracted from collagen gels after 48 hours were analyzed by flow cytometry for the following markers: CD14 **(B)**, BODIPY **(C)**, CD36 **(D)**, CD11b **(E)** and intracellular TNF **(F)**. Box and whisker plots show median, IQR and 1.5 standard deviations (Tukey plot). *p<0.05; **p<0.01 as determined by paired non-parametric two-tailed Wilcoxon rank sum test

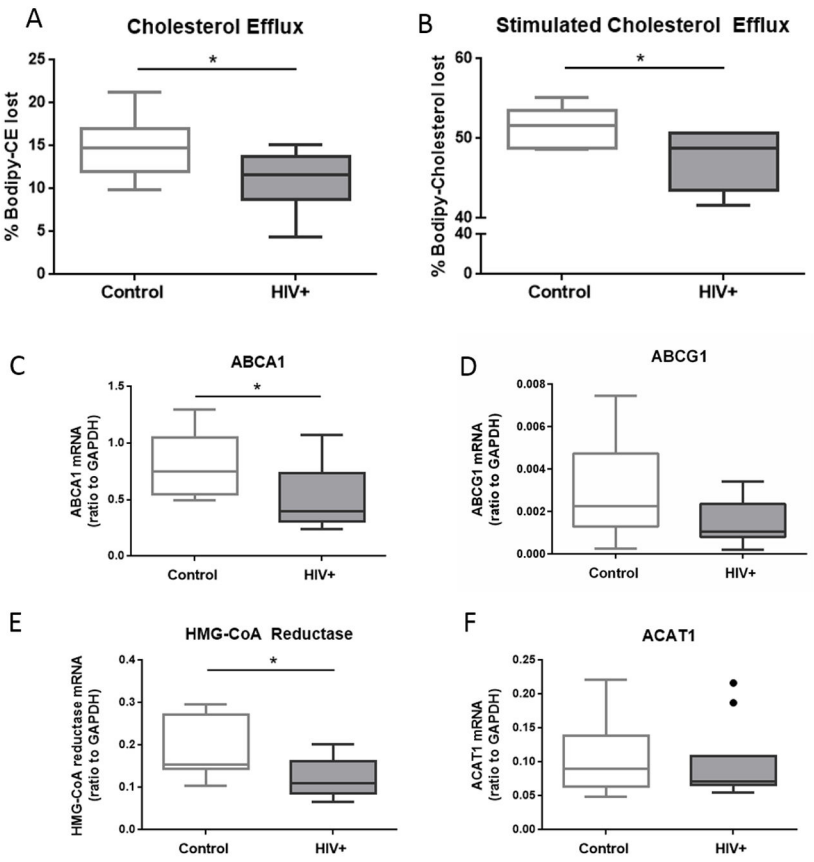

Figure 5. Monocytes from virologically-suppressed HIV+ donors show altered expression of cholesterol metabolism genes and impaired cholesterol efflux

PBMC from controls and virologically-suppressed HIV+ individuals (n=8 for each) were loaded with BODIPY-cholesterol and subsequent cholesterol efflux from monocytes was measured via flow cytometry. The percentage cholesterol efflux after 30 minutes (as a proportion of total loaded) is shown for experiments conducted in the absence **(A)** or presence **(B)** of the cholesterol accepter methyl-β-cyclodextrin. Gene expression of the cholesterol metabolism genes ABCA1 **(C)**, ABCG1 **(D)**, HMG-CoA reductase **(E)** and ACAT **(F)** was determined via qPCR analysis of mRNA isolated from purified monocytes from controls and virologically-suppressed HIV+ donors (n=11 in each group) and standardized to GAPDH expression. Box and whisker plots show median, IQR and 1.5 standard deviations (Tukey plot). Significance was tested using an unpaired two-tailed Mann Whitney U test, *$p<0.05$.